

RESEARCH LETTER

10.1002/2015GL067312

Key Points:

- New ionosphere model reveals source of midlatitude peak density structure
- Model three-peak structure agrees well with global satellite data
- Role of the prevailing neutral meridional wind flow

Supporting Information:

- Supporting Information S1
- Movie S1

Correspondence to:

N. Maruyama,
naomi.maruyama@noaa.gov

Citation:

Maruyama, N., Y.-Y. Sun, P. G. Richards, J. Middlecoff, T.-W. Fang, T. J. Fuller-Rowell, R. A. Akmaev, J.-Y. Liu, and C. Valladares (2016), A new source of the midlatitude ionospheric peak density structure revealed by a new Ionosphere-Plasmasphere model, *Geophys. Res. Lett.*, *43*, 2429–2435, doi:10.1002/2015GL067312.

Received 5 DEC 2015

Accepted 29 JAN 2016

Accepted article online 2 FEB 2016

Published online 31 MAR 2016

©2016. The Authors.

This is an open access article under the terms of the Creative Commons Attribution-NonCommercial-NoDerivs License, which permits use and distribution in any medium, provided the original work is properly cited, the use is non-commercial and no modifications or adaptations are made.

A new source of the midlatitude ionospheric peak density structure revealed by a new Ionosphere-Plasmasphere model

Naomi Maruyama^{1,2}, Yang-Yi Sun^{1,2,3}, Phillip G. Richards⁴, Jacques Middlecoff^{5,6}, Tzu-Wei Fang^{1,2}, Timothy J. Fuller-Rowell^{1,2}, Rashid A. Akmaev², Jaun-Yeng Liu³, and Cesar E. Valladares⁷

¹Cooperative Institute for Research in Environmental Sciences, University of Colorado at Boulder, Boulder, Colorado, USA, ²Space Weather Prediction Center, National Oceanic and Atmospheric Administration, Boulder, Colorado, USA, ³Institute of Space Science, National Central University, Taoyuan, Taiwan, ⁴Department of Physics and Astronomy, George Mason University, Fairfax, Virginia, USA, ⁵Cooperative Institute for Research in the Atmosphere, Colorado State University, Fort Collins, Colorado, USA, ⁶Global Systems Division, National Oceanic and Atmospheric Administration, Boulder, Colorado, USA, ⁷Institute for Scientific Research, Boston College, Chestnut Hill, Massachusetts, USA

Abstract The newly developed Ionosphere-Plasmasphere (IP) model has revealed neutral winds as a primary source of the “third-peak” density structure in the daytime global ionosphere that has been observed by the low-latitude ionospheric sensor network GPS total electron content measurements over South America. This third peak is located near -30° magnetic latitude and is clearly separate from the conventional twin equatorial ionization anomaly peaks. The IP model reproduces the global electron density structure as observed by the FORMOSAT-3/COSMIC mission. The model reveals that the third peak is mainly created by the prevailing neutral meridional wind, which flows from the summer hemisphere to the winter hemisphere lifting the plasma along magnetic field lines to higher altitudes where recombination is slower. The same prevailing wind that increases the midlatitude density decreases the low-latitude density in the summer hemisphere by counteracting the equatorial fountain flow. The longitudinal variation of the three-peak structure is explained by the displacement between the geographic and geomagnetic equators.

1. Introduction

The classical structure of the Earth’s daytime *F*-region ionosphere at midlatitude and low latitude is characterized by the two peaks of electron density on either side of the dip equator called the Appleton anomaly or the Equatorial Ionization Anomaly (EIA) [Hanson and Moffett, 1966; Schunk and Nagy, 2000]. The EIA is produced by a combination of the daytime upward $\mathbf{E} \times \mathbf{B}$ drift of plasma at the magnetic equator followed by downward diffusion along field lines to higher latitudes. Global GPS total electron content (TEC) observations usually show two EIA peaks since TEC tends to closely reflect the *F*-region peak density ($N_m F_2$) at midlatitude and low latitude. FORMOSAT-3/COSMIC (Constellation Observing System for Meteorology, Ionosphere and Climate) (F3/C) satellite measurements have led to significant improvement of our understanding of the global morphology and variability of the dynamical EIA structures [e.g., Lin et al., 2007; 2012]. Recently, the ground-based Low-Latitude Ionospheric Sensor Network (LISN) GPS TEC observations with high temporal and spatial resolution have revealed a new peak of TEC poleward of the conventional two EIA peaks over the American longitude sector at the December solstice [Valladares, 2013]. The main objective of this research is to investigate the causes and the global morphology and dynamics of the “three-peak structure” by simulations with a newly developed Ionosphere-Plasmasphere (IP) model. The global $N_m F_2$ from the IP simulation is validated by comparison to F3/C observations.

2. The Ionosphere-Plasmasphere (IP) Model

The Ionosphere-Plasmasphere (IP) model is a time-dependent, 3-D model of the ionosphere and plasmasphere. It provides time-dependent, global, three-dimensional plasma densities for nine ion species, electron and ion temperatures, and both parallel and perpendicular velocities of the ionosphere and plasmasphere. A unique feature of the IP model is global implementation of a more accurate representation of the Earth’s magnetic field in conjunction with the well-tested Field Line Interhemispheric Plasma (FLIP) model [Richards et al., 2010], using Apex coordinates [Richmond, 1995] that are based on the International Geomagnetic Reference Field (IGRF), as in the Global Ionosphere Plasmasphere (GIP) model [Fang et al., 2009]. The realistic representation of the Earth’s magnetic field

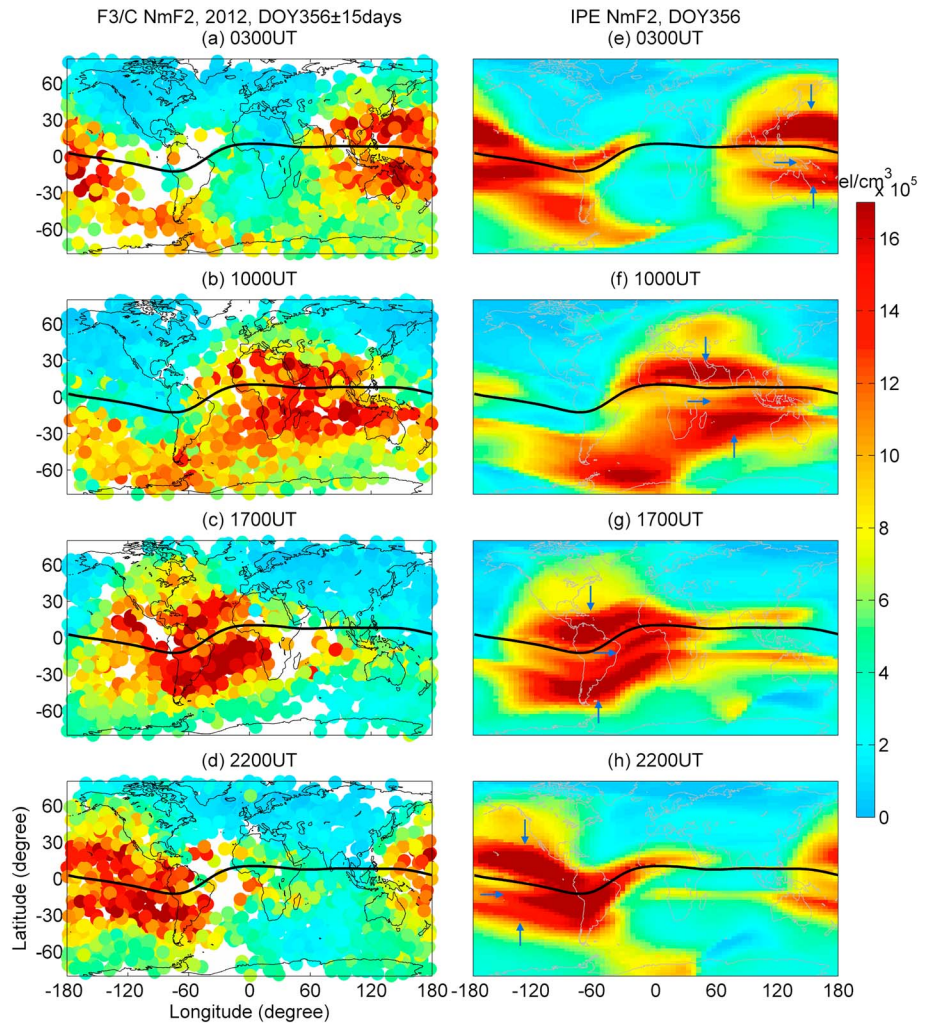


Figure 1. Comparison of the global N_mF_2 (10^5 cm^{-3}) between (a–d) F3/C measurements and (e–h) IP model simulation at 0300 UT (Figures 1a and 1e), 1000 UT (Figures 1b and 1f), 1700 UT (Figures 1c and 1g), and 2200 UT (Figures 1d and 1h) at the December solstice in 2012. The black solid curves display the geomagnetic equator. The three arrows in each IP simulation highlight the three-peak structure.

enables more accurate studies of the longitudinal and UT dependencies globally. Furthermore, implementation of a global static grid with a semi-Lagrangian scheme allows for the global seamless plasma transport perpendicular to the magnetic field lines [Fuller-Rowell *et al.*, 1987], as used in Coupled Thermosphere Ionosphere Model (CTIM) [Fuller-Rowell *et al.*, 1996] and Coupled Thermosphere Ionosphere Plasmasphere electrodynamics (CTIPe) model [Millward *et al.*, 2001]. The semi-Lagrangian scheme has the advantage of allowing for larger time steps than the Eulerian-based advection schemes [Staniforth and Côté, 1991], with no loss of accuracy.

These IP model simulations have a longitudinal resolution of 4.5° . The latitudinal resolution is variable and optimized to resolve the dynamical EIA feature with an average latitudinal resolution of $\sim 1.3^\circ$ poleward of ± 30 magnetic latitude and $\sim 0.34^\circ$ equatorward of $\pm 30^\circ$ magnetic latitude. The latitude of the most poleward flux tube is 88.2° . No altitude boundary is necessary because all the flux tubes are closed. The integration of the model equation calculation is carried out along all the closed field lines in the IP model, in order to avoid the potential artificial discontinuity created by the boundary conditions. The arc length between two grid points along the magnetic grid has been designed to be less than the plasma scale height in the *F*-region. The number of grid points along a field line ranges from 11 near the equator to 1115 at the highest latitude.

Because the model results are compared with monthly averaged data when magnetic activity was very low, the IP model uses empirical models as key inputs for this study. The thermospheric temperatures and number

densities are obtained from the Naval Research Laboratory Mass Spectrometer, Incoherent Scatter Radar Extended (NRLMSISE-00) model [Picone *et al.*, 2002]. The winds are from the Horizontal Wind Model (HWM93) [Hedin *et al.*, 1996]. The electric fields are provided by combining the low-latitude/midlatitude model of Scherliess and Fejer [1999] and the high-latitude model of Weimer [1996]. However, the IP model has an option to couple to the global ionospheric electrodynamic solver [Richmond and Maute, 2014], called the Ionosphere-Plasmasphere-Electrodynamics (IPE) model. Further detailed description of the IPE model is in a forthcoming paper.

3. Results and Discussion

Figure 1 compares the F3/C observations (Figures 1a–1d) and IP simulation (Figures 1e–1h) of the global N_mF_2 for the December solstice in 2012. The observations shown in Figures 1a–1d are hourly global distributions of the F3/C N_mF_2 accumulated over a month (day of year (DOY) 356 ± 15 days). The IP simulation reveals a very realistic representation of the global density observed by the F3/C (correlation coefficient = 0.84 as shown in Figure 2). The good longitudinal coverage, including over the ocean in the F3/C measurements, reveals the morphology of the global density. The solar and magnetic activity conditions during the observation period are shown in Figure 3. The average K_p was approximately 1 during this period. Local time effects are not important near solstice as the day-to-day changes in solar zenith angle variation are negligible. This along with the quiet solar and magnetic activity means a single simulation for day 365 can represent the conditions very well. The $F_{10.7}$ solar activity index was set to 120 and the geomagnetic activity to $A_p=4$. Auroral precipitation was not included in the IP model simulation, since it is likely to have little direct effect on the midlatitude and low-latitude structure under these conditions.

The three-peak structure identified in the IP simulation resembles the “Tropical Ionization Anomaly” (TIA) first observed in LISN GPS TEC [Valladares, 2013]. The third peak is located near -30° magnetic latitude in the summer hemisphere. It is clearly distinguished from the usual two peaks associated with the conventional EIA that appear on either side of the dip equator at around $\pm 15^\circ$ magnetic latitude. The third peak can remain throughout the night in some longitude sectors (e.g., Figures 1b and 1f). The density of the third peak can also become larger than the summer EIA peak (e.g., Figures 1b, 1c, 1f and 1g). The Weddell Sea Anomaly [Sun *et al.*, 2015] appears near the Argentine Islands at 1000 UT in Figures 1b and 1f. The third peak continues to expand in both latitude and longitude and by 1700 UT reaches the maximum density over Argentina. The lack of latitudinal spatial resolution makes it difficult to clearly identify the third peak in the summer hemisphere in the F3/C observations (Figures 1a–1d), although hemispheric asymmetry is apparent.

The three-peak structure in the electron density obtained from the IP simulation is demonstrated at local noon in Figure 4a at 1700 UT (corresponding to Figure 1g). The third peak near -30° magnetic latitude is mainly created by the prevailing neutral meridional wind from the summer hemisphere to the winter hemisphere lifting the plasma along magnetic field lines to a higher altitude where recombination is slower. The field-aligned wind at the same longitude sector in Figure 4b is mostly northward (equatorward) in the summer hemisphere during the few hours preceding 1700 UT. On the dayside this prevailing flow is counteracted by the daily wind pattern (diurnal tide) directed poleward from the subsolar latitude. At solstice, the diurnal tidal effect is minimized near the subsolar latitude in the summer hemisphere (-23° geographic latitude) near the summer EIA peak in the American sector (-25° geographic latitude). The same equatorward wind that increases the midlatitude density decreases the low-latitude EIA crest density in the summer hemisphere, by transporting plasma equatorward, against the usual EIA plasma fountain flow. The explanation with regard to the equatorward shift of the EIA peak by equatorward wind is consistent with previous studies including Rishbeth [1972] based on the theoretical analysis of the stationary solution of the continuity equation for the electron density [Bramley and Young, 1968] and Nanan *et al.* [2012] based on more sophisticated numerical simulations by using a physics-based model. Indeed, the mechanism for the third-peak formation is confirmed by the simulations showing that the density of the third-peak density becomes larger and the density of the Southern EIA crest becomes smaller with the peak location shifted equatorward if the wind input to the IP model is artificially doubled (results not shown). The different responses to the same equatorward wind can be attributed simply to the fact that the magnetic field lines are tilted at midlatitude, whereas they are almost horizontal near the equator. The good agreement between F3/C observations and IP simulation supports the validity of the NRLMSISE-00, HWM93, and electric field empirical models under these

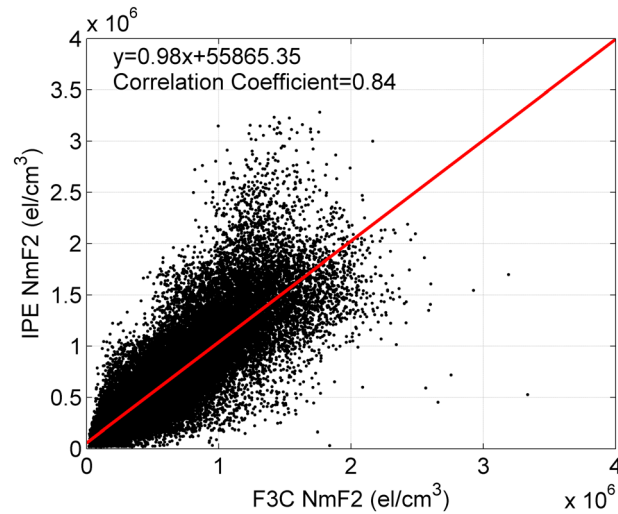


Figure 2. Correlation between the F3/C observation and IP simulation.

quiet conditions at the December solstice in 2012. The summer to winter prevailing wind from the HWM93 model is particularly important for the formation of the third density peak.

The three-peak structure exhibits large longitudinal variations, as shown in Figure 5, where the UT (longitudinal) variations of the noon N_mF_2 latitudinal profiles obtained from the IP simulation are displayed. The third-peak density at -30° magnetic latitude is larger than that of the summer EIA peak at -15° magnetic latitude, by a factor of about 1.5 at 1700 UT. The third peak maximizes at around 1700 UT (corresponding to Figure 1g) over the American longitude sector (-77° geographic

longitude), whereas the minimum value of the third peak is found at around 1000 UT when local noon is in the African sector (corresponding to Figure 1f). The daytime wind pattern directed poleward is minimized near the summer EIA peak in the American longitude sector as compared to other sectors since the American longitude sector has the largest displacement between geomagnetic and geographic equators. This explains the longitudinal variation of the third peak in Figure 5.

The fourth peak that appears at -45° magnetic latitude in the 1000 UT profile is larger than the third peak. Furthermore, Figure 1 shows the fourth daytime peak density near $45-50^\circ$ geographic latitude in the Northern Hemisphere at other longitudes that is much larger than that of the American longitude sector, although the electron density is much smaller than that of the major three-peak structure. Whether or not the third and fourth peaks are correlated is an interesting science question, which is beyond the scope of this paper and will be investigated in our forthcoming paper, along with longitudinal, seasonal, solar and magnetic activity, and yearly variations.

4. Conclusions

The morphology and dynamics of the global three-peak structure have been reproduced by the newly developed IP model for the December solstice in 2012. The three-peak structure has been observed in the LISN GPS TEC over the South American continent. The conventional understanding of the midlatitude and low-latitude daytime ionosphere is that there are two peaks of the Equatorial Ionization Anomaly that are caused by a combination of the daytime upward $\mathbf{E} \times \mathbf{B}$ drift lifting the plasma to a region of decreased recombination followed by downward diffusion along field lines to around $\pm 15^\circ$ magnetic latitude. The IP simulation successfully captures the spatial and temporal variations of the global density observed by the F3/C mission.

The main features of the three-peak structure obtained from the IP model are summarized as follows: The third peak, which is located near -30° magnetic latitude, can have a larger density than the summer EIA peak. The third peak can even be observed throughout the night in some longitude sectors. The three-peak structure shows considerable longitudinal variation. Its density maximizes around 1700 UT over the South American longitude sector and has a minimum around 1000 UT over the African sector.

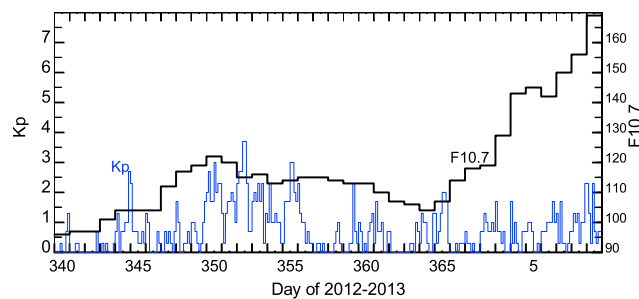


Figure 3. Solar and magnetic activity conditions during the period corresponding to the F3/C observations (DOY 356 ± 15 days 2012). The black line shows the daily values of $F_{10.7}$ index, while the blue line shows K_p index.

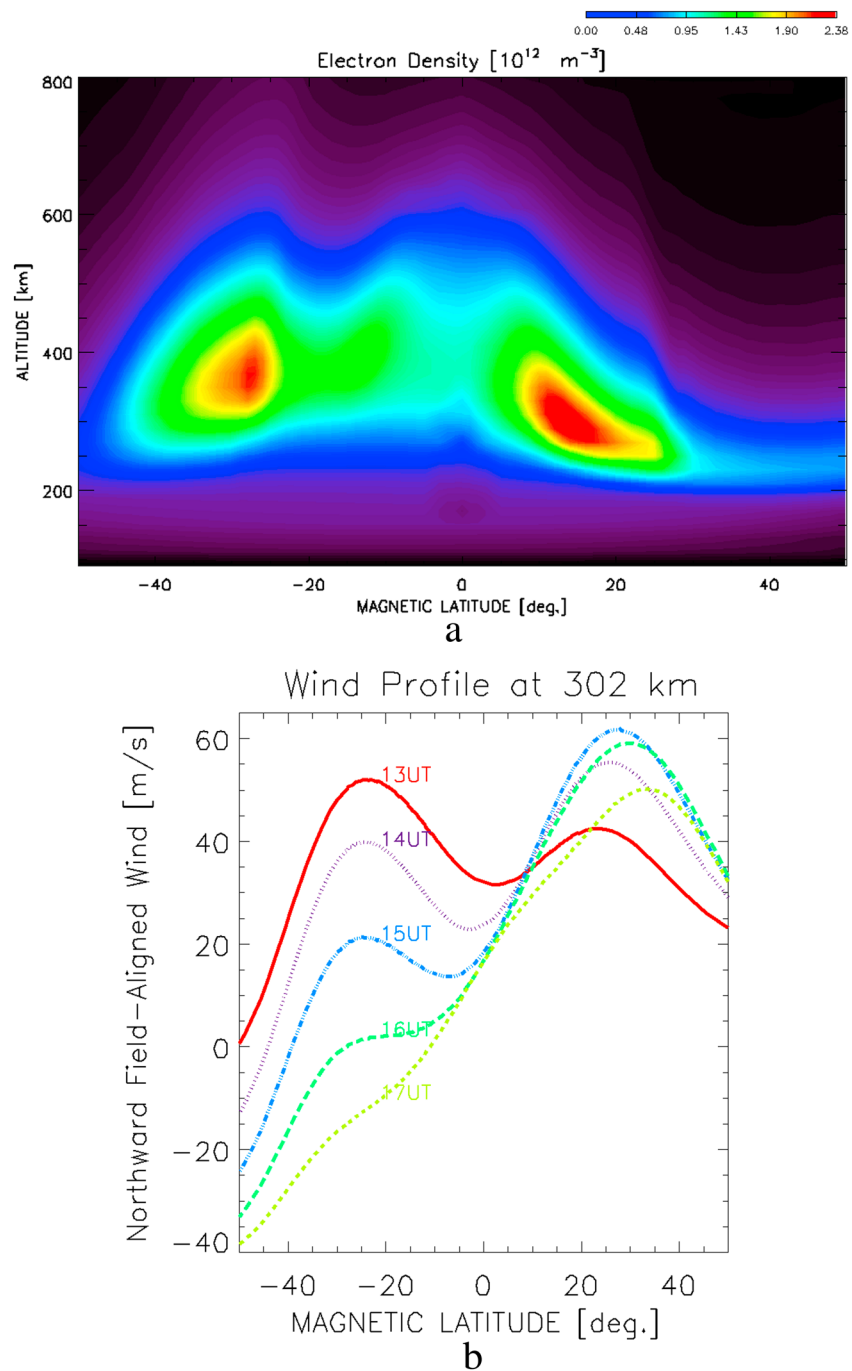


Figure 4. (a) Three-peak structure reproduced in the electron density (10^{12} m^{-3}) obtained from the IP model simulation at local noon at 283° geographic longitude at 1700 UT (corresponding to Figure 1g). (b) Universal Time variation of the field-aligned wind used in the simulation at 302 km altitude at the corresponding longitude to Figure 4a. Positive northward, parallel to the magnetic field. The field-aligned wind is mostly northward (equatorward) in the summer hemisphere before 1700 UT.

The summer to winter hemisphere prevailing neutral meridional wind is mainly responsible for the third peak as it lifts the plasma to higher altitudes where recombination is slower. On the dayside, this prevailing flow is counteracted by the daily wind pattern directed poleward from the subsolar latitude. At the solstice, the diurnal tidal effect is minimized near the subsolar latitude in the summer hemisphere. The longitudinal variation of the three-peak structure is related to the longitudinal variation of the displacement between the geographic and geomagnetic equators.

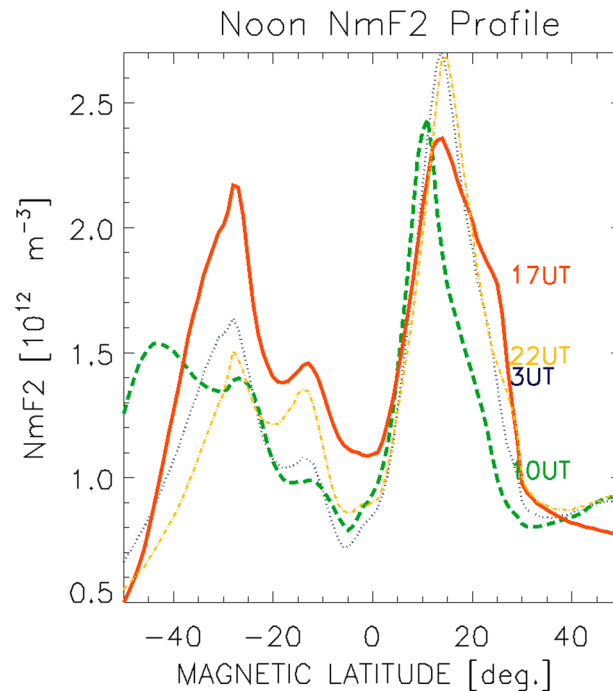


Figure 5. Universal time (longitudinal) variations of the three-peak structure revealed in the local noon NmF_2 (10^{12} m^{-3}) latitudinal profiles. Individual lines of 0300 UT, 1000 UT, 1700 UT, and 2200 UT correspond to 136° , 30.5° , 283° , and 208° geographic longitudes, respectively, corresponding to Figures 1e–1h.

It has long been understood that the low-latitude ionosphere has been the region in which the $\mathbf{E} \times \mathbf{B}$ drift dominates plasma dynamics, whereas the midlatitude ionosphere has been the region in which the neutral wind dominates. The results from this model study on the interconnection between the neutral wind and ionospheric plasma structure indicate that the boundary between the two regimes can be significantly altered under solstice conditions due to a combination of the reduced $\mathbf{E} \times \mathbf{B}$ drift and enhanced prevailing wind. In the future, the thermospheric neutral winds may be estimated from knowing the ionospheric plasma structure. The good agreement between our new IP model and F3/C observations and the reproduction of the three-peak structure in particular is a significant advance in our ionosphere modeling capability, which promises valuable potential use for future science investigations and space weather forecasting capabilities.

Acknowledgments

This material is based upon work supported by the National Science Foundation (NSF grant ATM-1103149, ATM-1042258, and ATM-1452298), NASA awards NNX13AF77G and NNX16AB83G to the University of Colorado at Boulder, and the Taiwan National Science Council (NSC) grant NSC 102-2628-M-008-001. The authors thank COSMIC Data Analysis and Archival Center (CDAAC) and Taiwan Analysis Center for COSMIC (TACC) for making the F3/C data available online. Cesar E. Valladares was partially supported by Air Force Research Laboratory contract FA8718-09-C-0041, NSF grants ATM-1135675 and ATM-1242476, and NASA LWS grant NNX11AP02G. Phillip G. Richards was supported by NASA grant NNX15AI90G to George Mason University.

References

- Bramley, E. N., and M. Young (1968), Winds and electromagnetic drifts in the equatorial F2-region, *J. Atmos. Terr. Phys.*, *30*, 99–111, doi:10.1016/0021-9169(68)90044-5.
- Fang, T.-W., H. Kil, G. Millward, A. D. Richmond, J.-Y. Liu, and S.-J. Oh (2009), Causal link of the wave-4 structures in plasma density and vertical plasma drift in the low-latitude ionosphere, *J. Geophys. Res.*, *114*, A10315, doi:10.1029/2009JA014460.
- Fuller-Rowell, T., D. Rees, S. Quegan, R. Moffett, and G. Bailey (1987), Interactions between neutral thermospheric composition and the polar ionosphere using a coupled ionosphere-thermosphere model, *J. Geophys. Res.*, *92*(A7), 7744–7748, doi:10.1029/JA092iA07p07744.
- Fuller-Rowell, T. J., D. Rees, S. Quegan, R. J. Moffett, M. V. Codrescu, and G. H. Millward (1996), A coupled thermosphere-ionosphere model (CTIM), in *STEP Handbook of Ionospheric Models*, edited by R. W. Schunk, pp. 217–238, Utah State Univ, Logan.
- Hanson, W. B., and R. J. Moffett (1966), Ionization transport effects in the equatorial F region, *J. Geophys. Res.*, *71*, 5559–5572, doi:10.1029/JZ071i023p05559.
- Hedin, A. E., et al. (1996), Empirical wind model for the upper, middle and lower atmosphere, *J. Atmos. Terr. Phys.*, *58*, 1421–1447, doi:10.1016/0021-9169(95)00122-0.
- Lin, C. H., W. Wang, M. E. Hagan, C. C. Hsiao, T. J. Immel, M. L. Hsu, J. Y. Liu, L. J. Paxton, T. W. Fang, and C. H. Liu (2007), Plausible effect of atmospheric tides on the equatorial ionosphere observed by the FORMOSAT-3/COSMIC: Three-dimensional electron density structures, *Geophys. Res. Lett.*, *34*, L11112, doi:10.1029/2007GL029265.
- Lin, C. H., J. T. Lin, L. C. Chang, J. Y. Liu, C. H. Chen, W. H. Chen, H. H. Huang, and C. H. Liu (2012), Observations of global ionospheric responses to the 2009 stratospheric sudden warming event by FORMOSAT-3/COSMIC, *J. Geophys. Res.*, *117*, A06323, doi:10.1029/2011JA017230.
- Millward, G. H., I. C. F. Müller-Wodarg, A. Aylward, T. J. Fuller-Rowell, A. D. Richmond, and R. J. Moffett (2001), An investigation into the influence of tidal forcing on F region equatorial vertical ion drift using a global ionosphere-thermosphere model with coupled electrodynamics, *J. Geophys. Res.*, *106*(A11), 24,733–24,744, doi:10.1029/2000JA000342.
- Nanan, B., C. Y. Chen, P. K. Rajesh, J. Y. Liu, and G. J. Bailey (2012), Modeling and observations of the low latitude ionosphere-plasmasphere system at long deep solar minimum, *J. Geophys. Res.*, *117*, A08316, doi:10.1029/2012JA017846.
- Picone, J. M., A. E. Hedin, D. P. Drob, and A. C. Aikin (2002), NRLMSISE-00 empirical model of the atmosphere: Statistical comparisons and scientific issues, *J. Geophys. Res.*, *107*(A12), 1468, doi:10.1029/2002JA009430.
- Richards, P. G., R. R. Meier, and P. J. Wilkinson (2010), On the consistency of satellite measurements of thermospheric composition and solar EUV irradiance with Australian ionosonde electron density data, *J. Geophys. Res.*, *115*, A10309, doi:10.1029/2010JA015368.
- Richmond, A. D. (1995), Ionospheric electrodynamics using magnetic apex coordinates, *J. Geomagn. Geoelectr.*, *47*, 191–212.
- Richmond, A. D., and A. Maute (2014), Ionospheric electrodynamics modeling, in *Modeling the Ionosphere-Thermosphere*, *Geophys. Monogr. Ser.*, vol. 201, edited by J. D. Huba et al., AGU, Washington, D. C., doi:10.1002/9781118704417.
- Rishbeth, H. (1972), Thermospheric winds and the F region: A review, *J. Atmos. Terr. Phys.*, *34*, 1–47.
- Scherliess, L., and B. G. Fejer (1999), Radar and satellite global equatorial F region vertical drift model, *J. Geophys. Res.*, *104*(A4), 6829–6842, doi:10.1029/1999JA900025.
- Schunk, R. W., and A. F. Nagy (2000), *Ionospheres: Physics, Plasma Physics, and Chemistry*, *Cambridge Atmospheric and Space Sci. Ser.*, Cambridge Univ. Press, Cambridge.

- Staniforth, A., and J. Côté (1991), Semi-Lagrangian integration schemes for atmospheric models—A review, *Mon. Weather Rev.*, *119*, 2206–2223, doi:10.1175/1520-0493(1991)119<2206:SLISFA>2.0.CO;2.
- Sun, Y.-Y., T. Matsuo, N. Maruyama, and J.-Y. Liu (2015), Field-aligned neutral wind bias correction scheme for global ionospheric modeling at midlatitudes by assimilating FORMOSAT-3/COSMIC $h_m F_2$ data under geomagnetically quiet conditions, *J. Geophys. Res. Space Physics*, *120*, 3130–3149, doi:10.1002/2014JA020768.
- Valladares, C. E. (2013), LISN: Measurement of TEC values, and TID characteristics over South and Central America, Abstract SA12A-06 presented at 2013 Fall Meeting, AGU, San Francisco, Calif., 9–13 Dec.
- Weimer, D. R. (1996), A flexible IMF dependent model of the high-latitude electric potentials having “space weather” application, *Geophys. Res. Lett.*, *23*, 2549–2552, doi:10.1029/96GL02255.